

Supplementary information for

The linkers in fluorene-labeled 2'-deoxyuridines affect fluorescence discriminating phenomena upon duplex formation

So Young Lee,^a Seung Woo Hong,^a Hyeonuk Yeo^{*b} and Gil Tae Hwang^{*a}

^a Department of Chemistry and Green-Nano Materials Research Center, Kyungpook National University, Daegu 41566, Republic of Korea

^b Department of Chemistry Education, Kyungpook National University, Daegu 41566, Republic of Korea

Contents

Fig. S1. (a) Absorption and (b) emission spectra of U^F , U^{FL} and U^{DF} in MeOH at 25 °C	S2
Fig. S2. Ground-state optimized molecular structures of (a) U^F , (b) U^{FL} and (c) U^{DF}	S3
Fig. S3. Excited-state optimized molecular structures of (a) U^F , (b) U^{FL} and (c) U^{DF}	S3
Table S1. MALDI-TOF mass spectral data of ODNs containing U^F and U^{DF}	S4
Fig. S4. ¹ H NMR spectrum of U^F in CD ₃ OD	S6
Fig. S5. ¹ H NMR spectrum of 5 in CDCl ₃	S7
Fig. S6. ¹ H NMR spectrum of 6 in CDCl ₃	S8
Fig. S7. ¹ H NMR spectrum of U^{DF} in DMSO- <i>d</i> ₆	S9
Fig. S8. ¹ H NMR spectrum of 7 in CDCl ₃	S10
Fig. S9. ¹ H NMR spectrum of 8 in CDCl ₃	S11
Fig. S10. ¹ H NMR spectrum of 9 in CDCl ₃	S12
Fig. S11. ¹ H NMR spectrum of 10 in DMSO- <i>d</i> ₆	S13

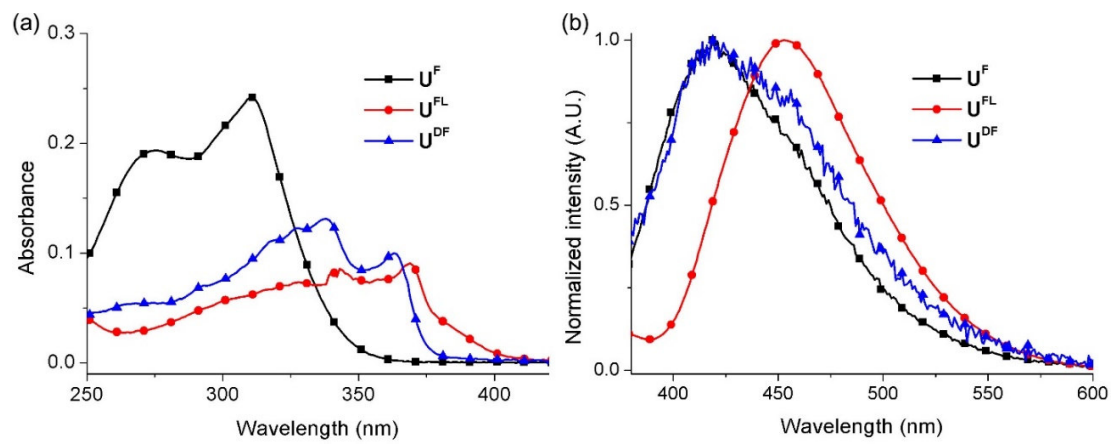


Fig. S1. (a) Absorption and (b) emission spectra of $\mathbf{U}^{\mathbf{F}}$, $\mathbf{U}^{\mathbf{FL}}$ and $\mathbf{U}^{\mathbf{DF}}$ in MeOH at 25 °C (each at a concentration of 3 μM). Excitation wavelengths: 310 nm for $\mathbf{U}^{\mathbf{F}}$, 369 nm for $\mathbf{U}^{\mathbf{FL}}$ and 363 nm for $\mathbf{U}^{\mathbf{DF}}$.

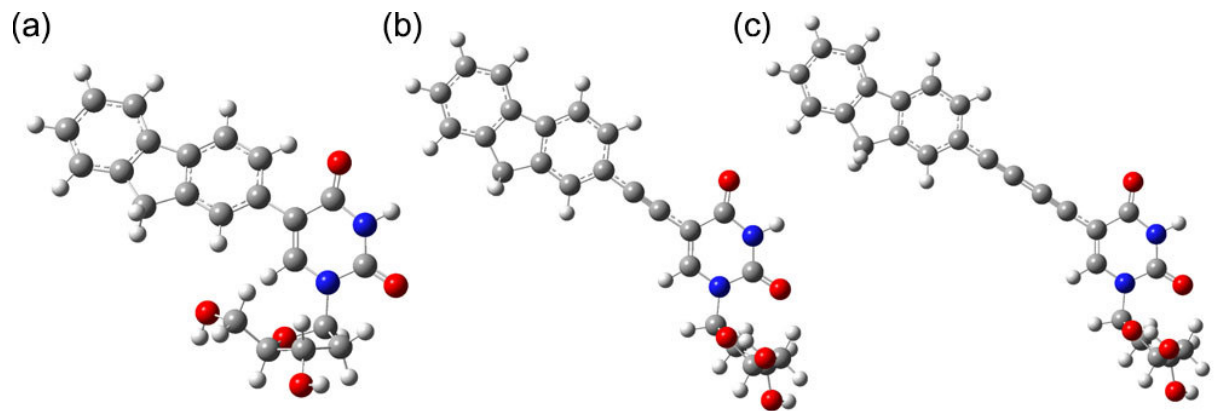


Fig. S2. Ground-state optimized geometries of (a) $\mathbf{U}^{\mathbf{F}}$, (b) $\mathbf{U}^{\mathbf{FL}}$ and (c) $\mathbf{U}^{\mathbf{DF}}$, calculated using density functional theory (DFT) at the B3LYP/6-31 level, in vacuo.

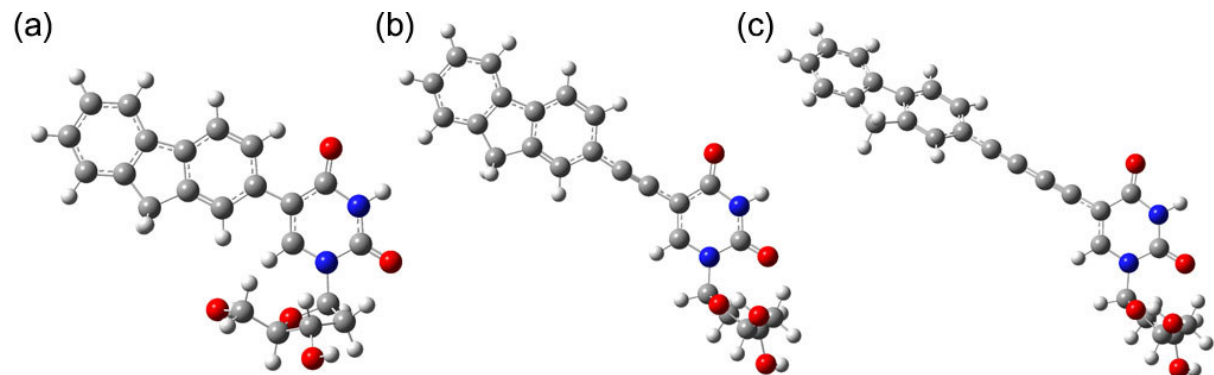
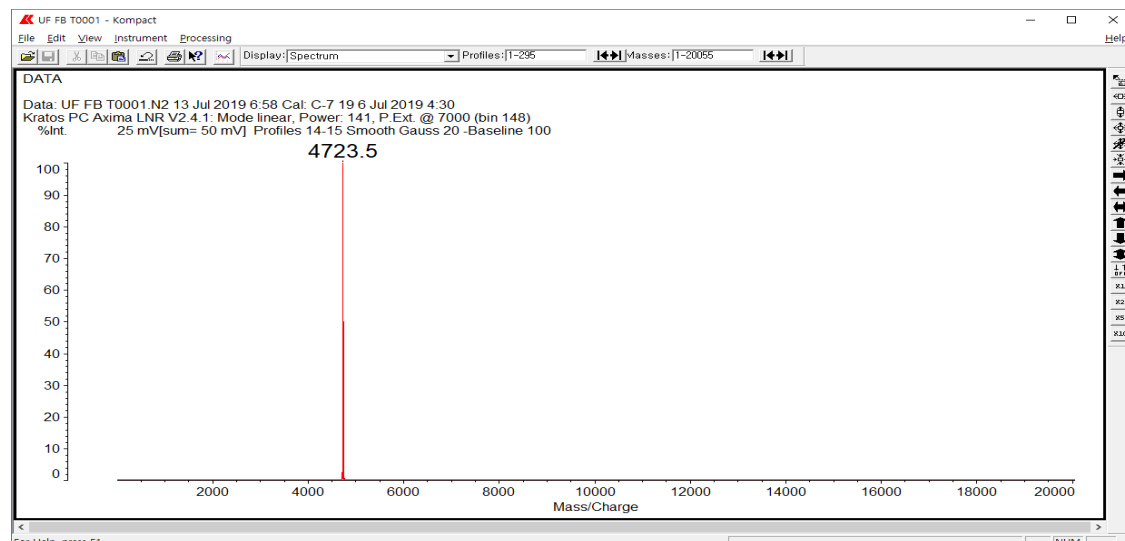


Fig. S3. Excited-state optimized geometries of (a) $\mathbf{U}^{\mathbf{F}}$, (b) $\mathbf{U}^{\mathbf{FL}}$ and (c) $\mathbf{U}^{\mathbf{DF}}$, calculated using density functional theory (DFT) at the B3LYP/6-31 level, in vacuo.

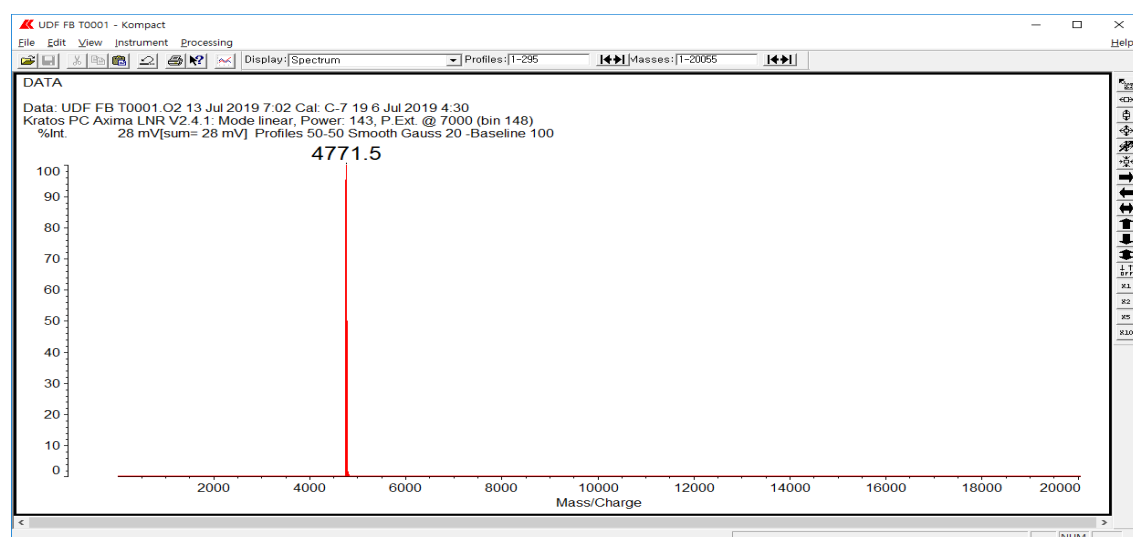
Table S1. MALDI-TOF mass spectral data of ODNs containing U^{F} and U^{DF}

ODN	Sequence	<i>m/z</i> found (calcd) for $[\text{M} + \text{H}]^+$
ODN1(U^{F})	5'-d(TGG ACT TU ^F T TCA ATG)-3'	4723.5 (4723)
ODN1(U^{DF})	5'-d(TGG ACT TU ^{DF} T TCA ATG)-3'	4771.5 (4771)
ODN2(U^{F})	5'-d(TGG ACT CU ^F C TCA ATG)-3'	4693.3 (4693)
ODN2(U^{DF})	5'-d(TGG ACT CU ^{DF} C TCA ATG)-3'	4740.3 (4741)

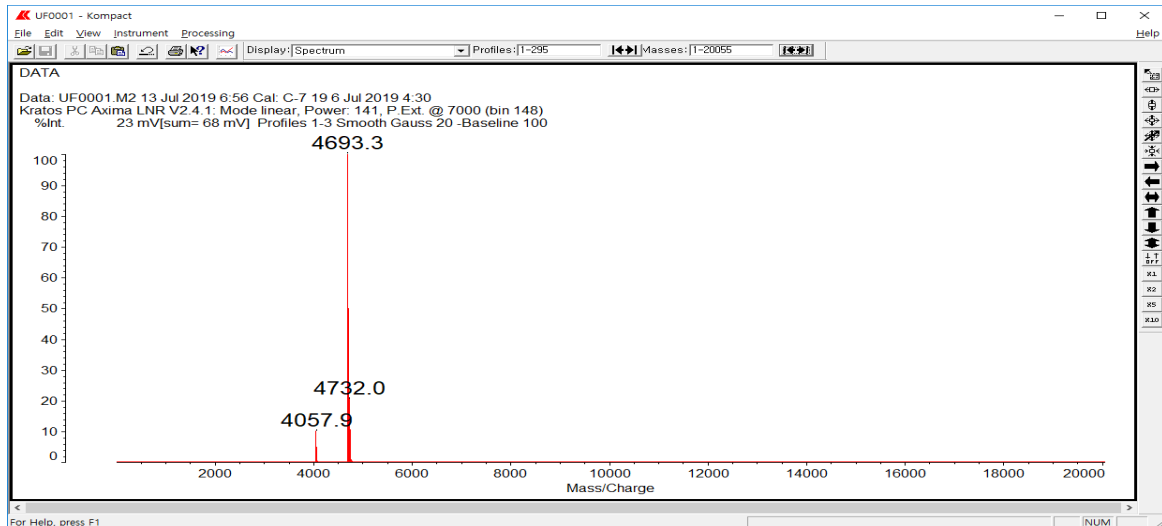
ODN1(U^{F})



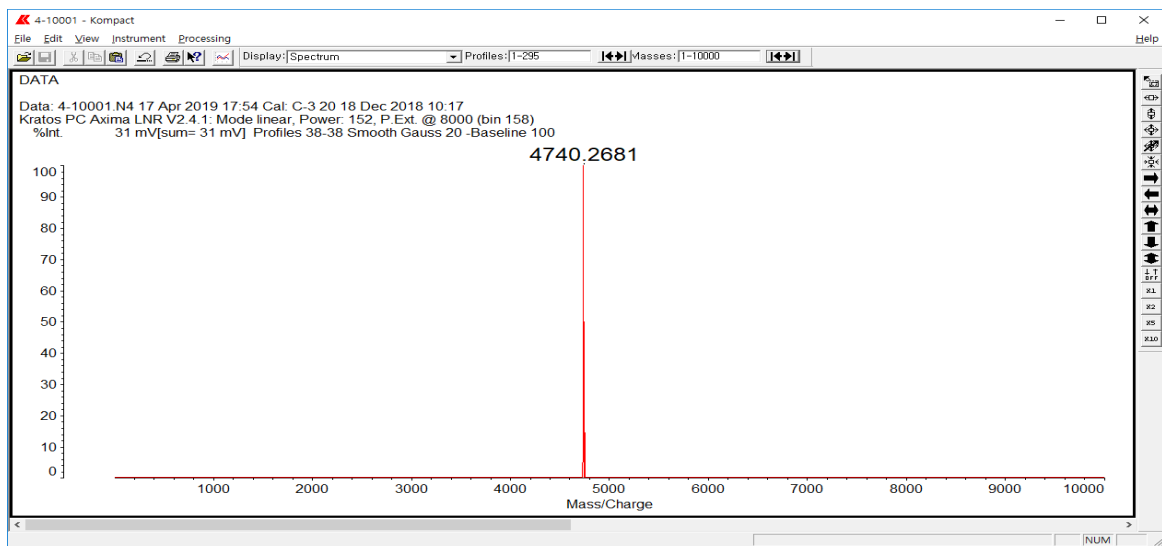
ODN1(U^{DF})



ODN2(\mathbf{U}^F)



ODN2(\mathbf{U}^{DF})



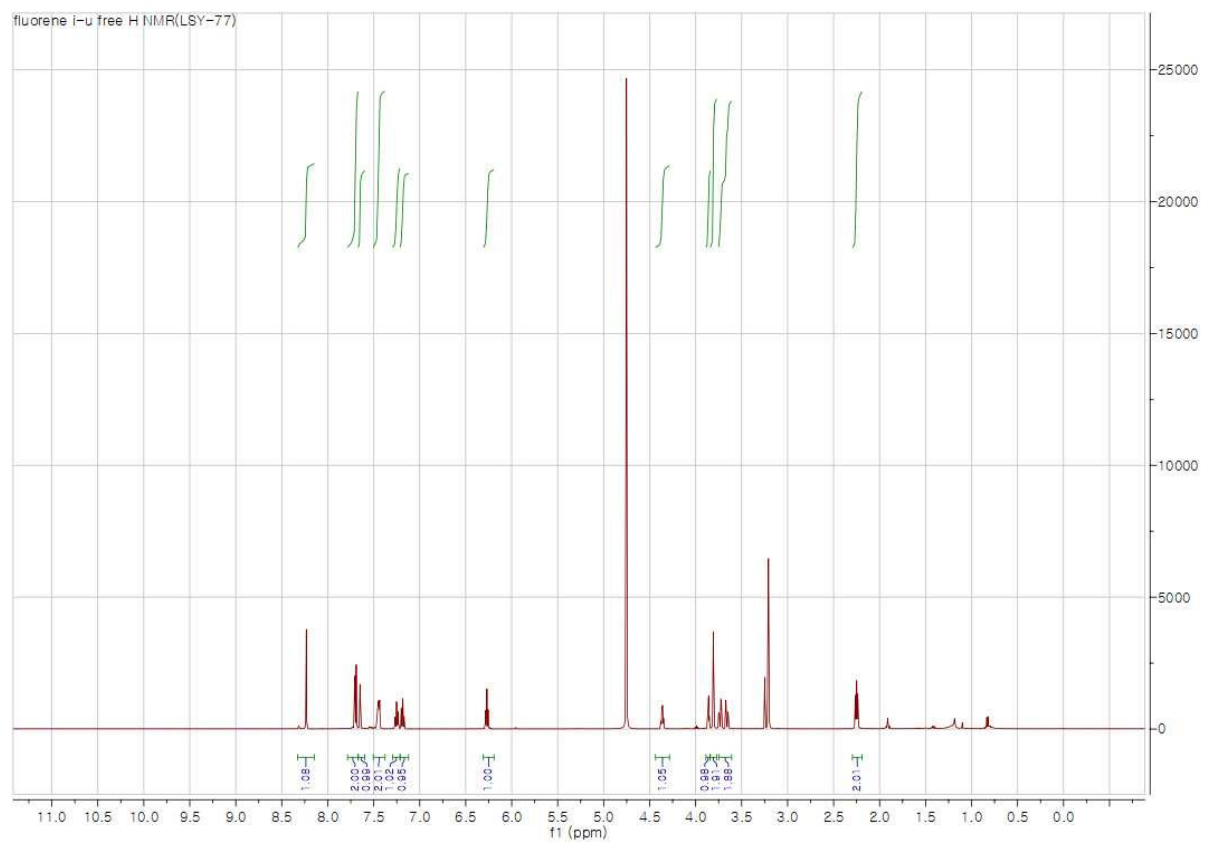


Fig. S4. ^1H NMR spectrum of \mathbf{U}^{F} in CD_3OD .

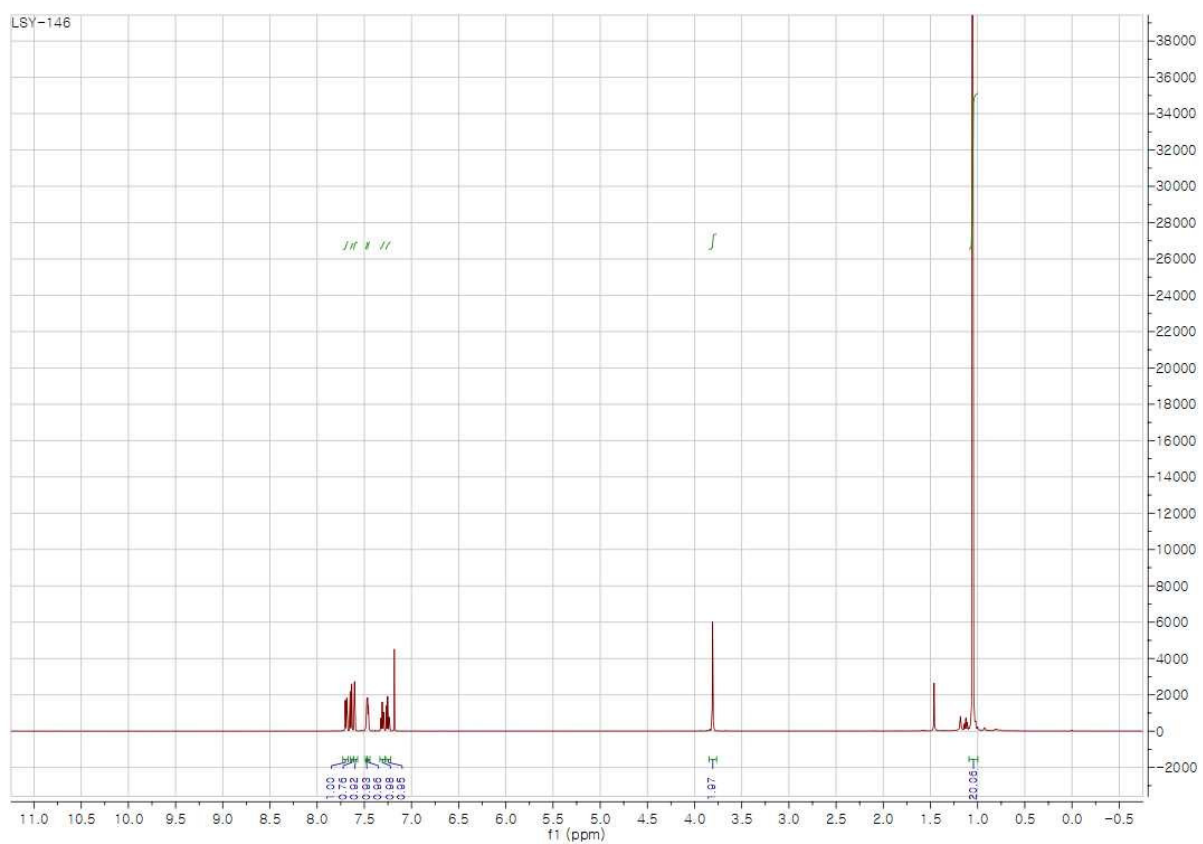


Fig. S5. ^1H NMR spectrum of **5** in CDCl_3 .

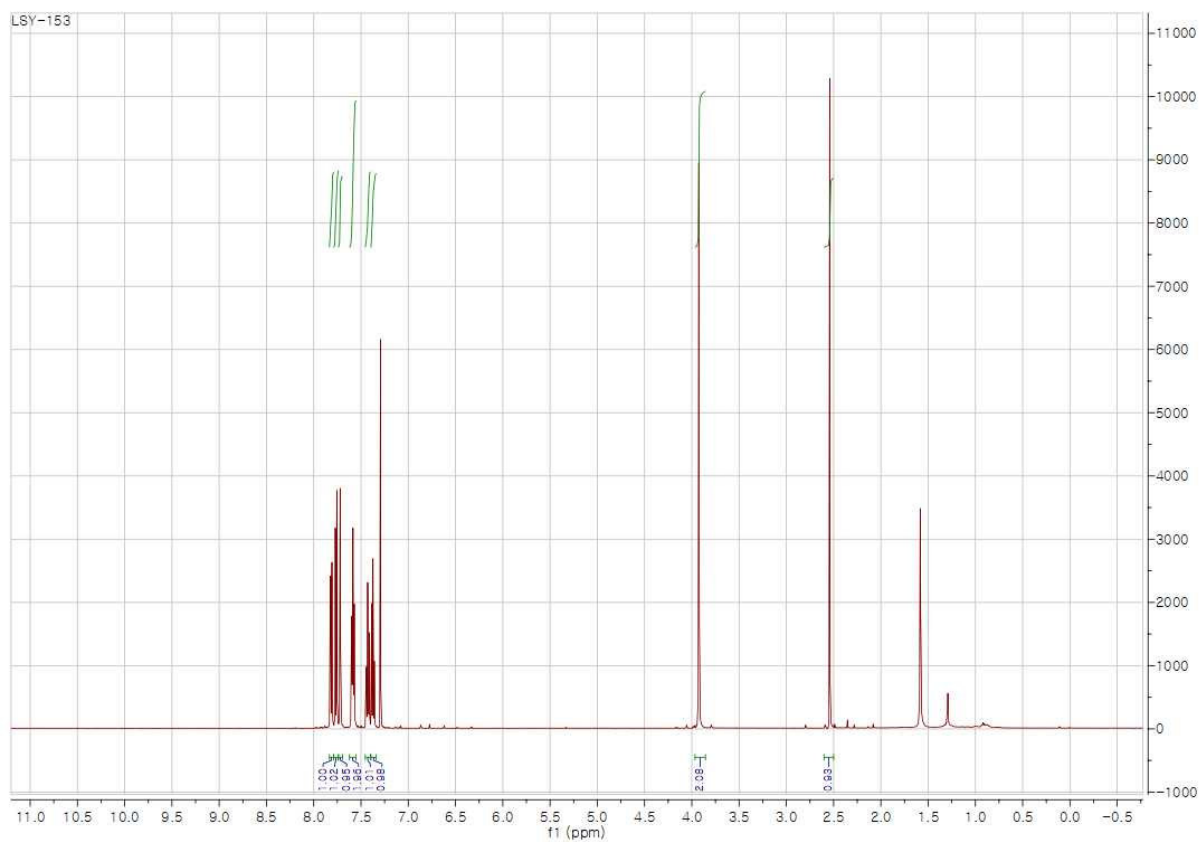


Fig. S6. ^1H NMR spectrum of **6** in CDCl_3 .

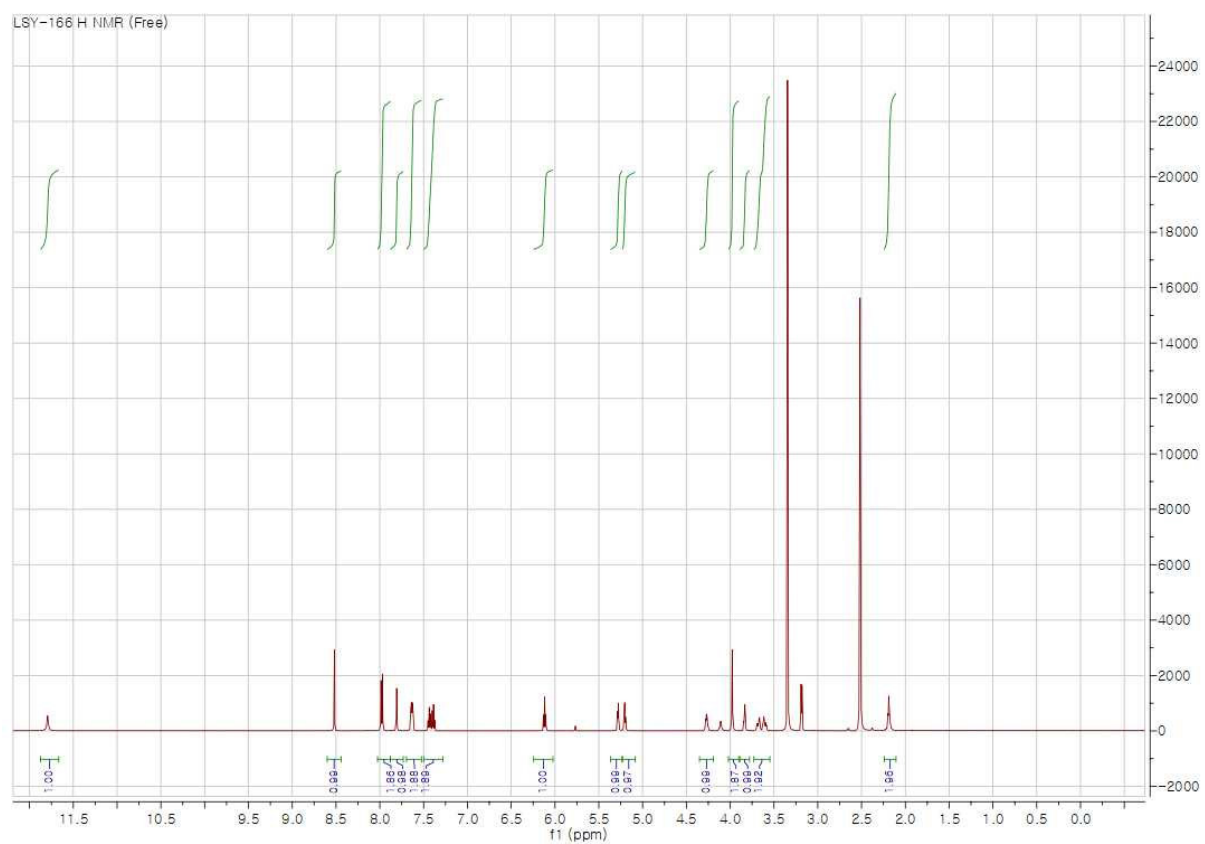


Fig. S7. ¹H NMR spectrum of **U^{PF}** in $\text{DMSO}-d_6$.

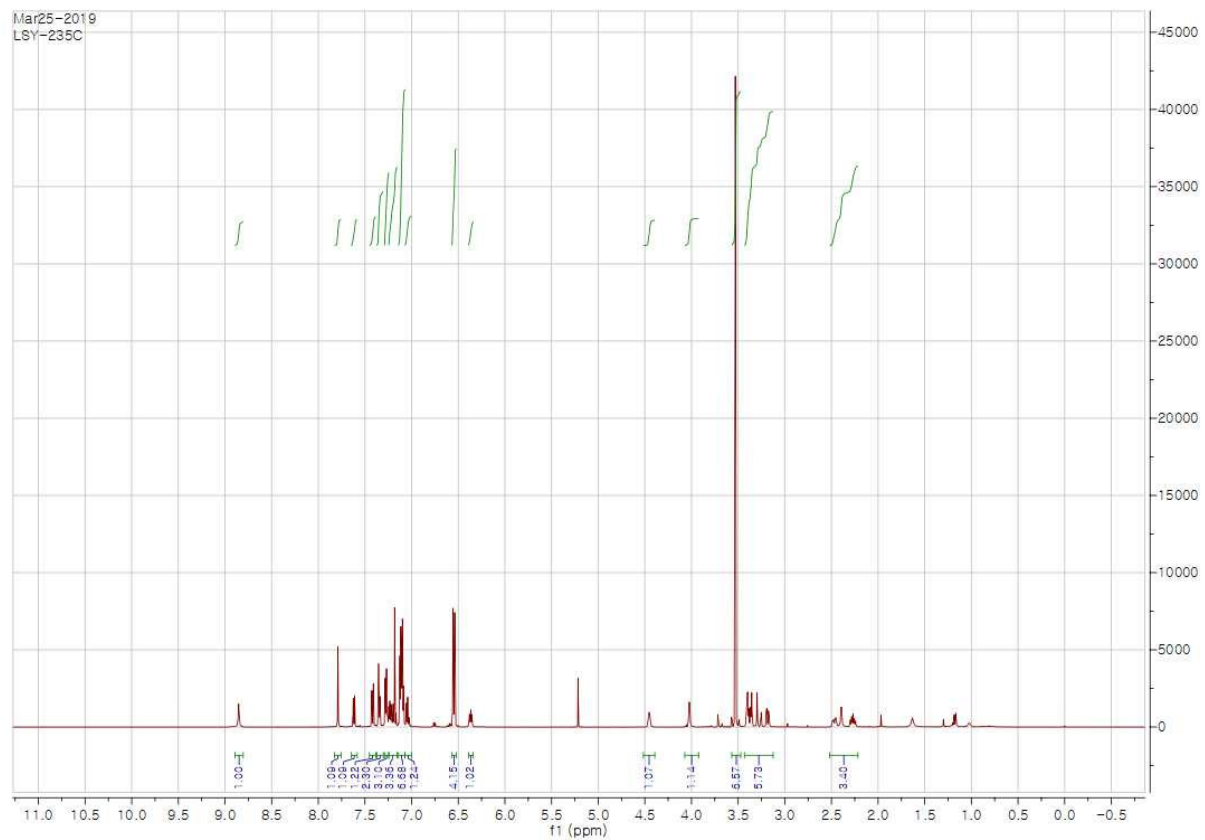


Fig. S8. ¹H NMR spectrum of **7** in CDCl₃.

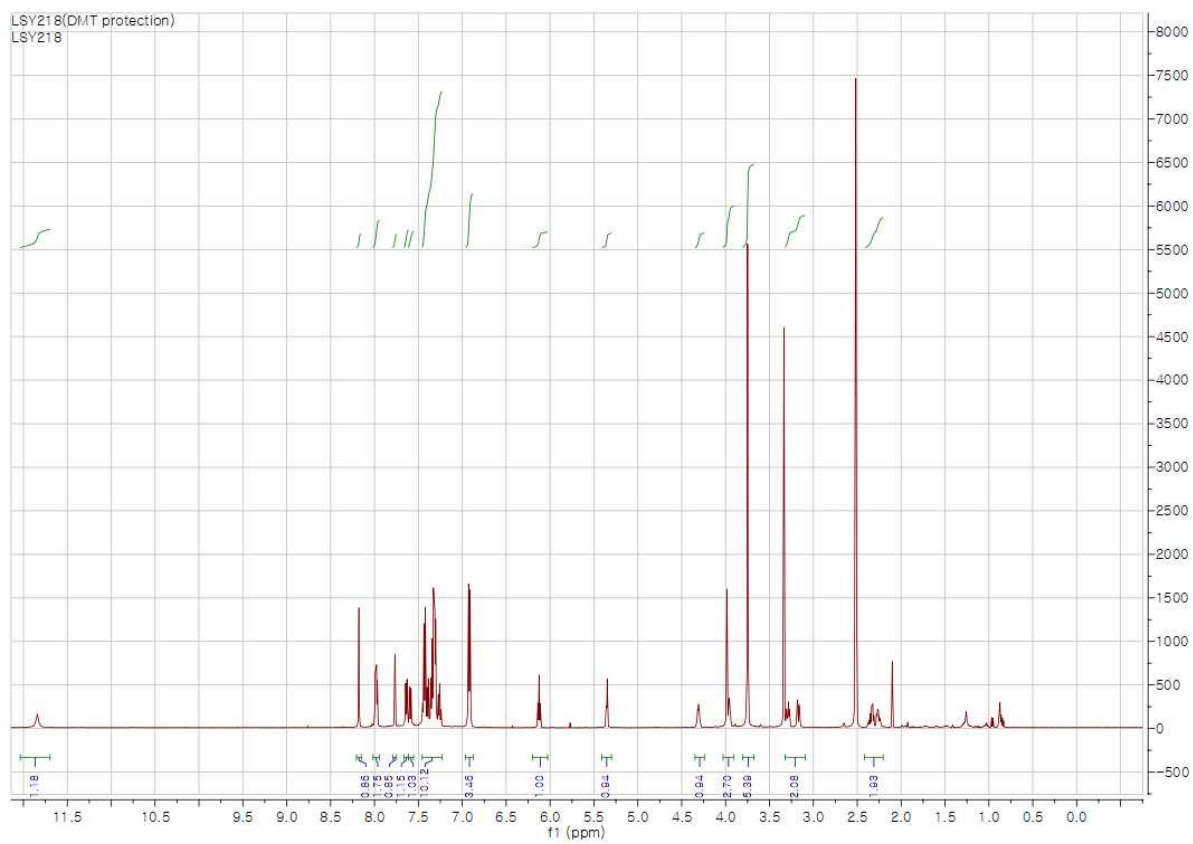


Fig. S9. ^1H NMR spectrum of **8** in CDCl_3 .

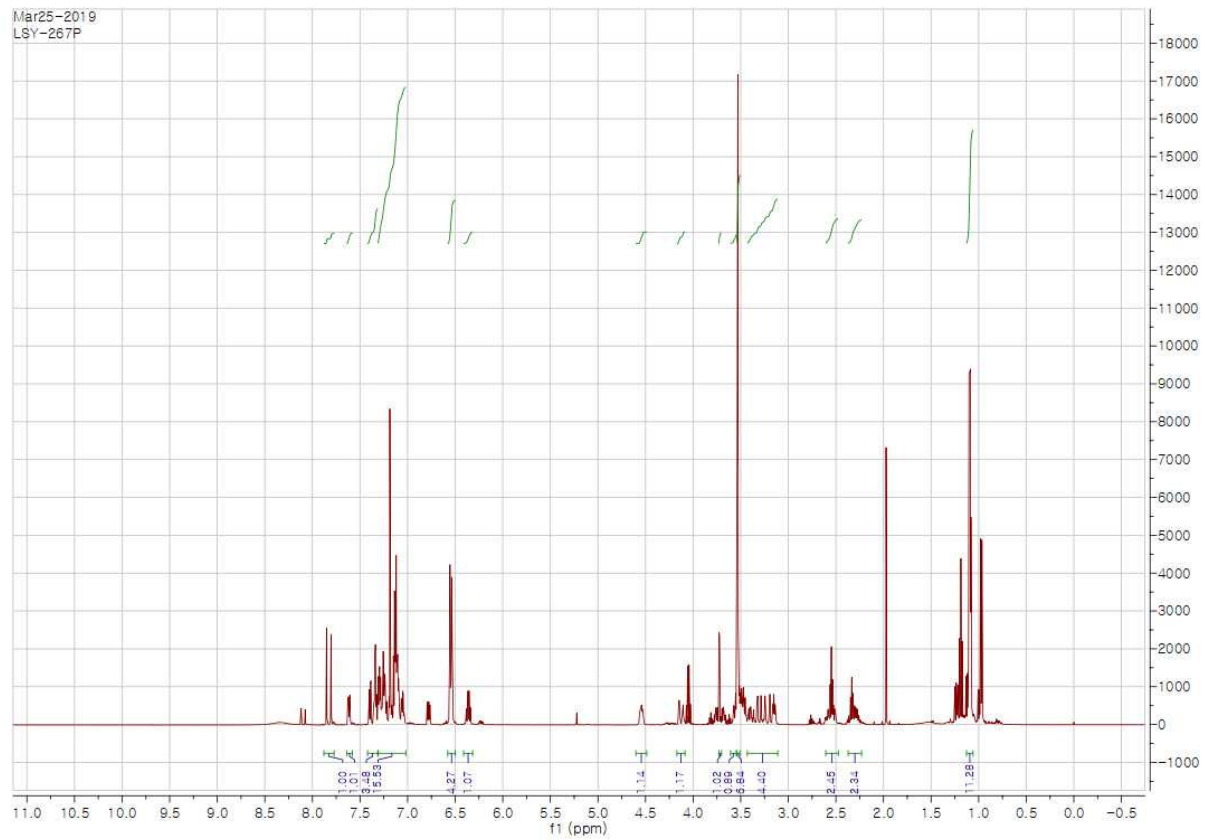


Fig. S10. ^1H NMR spectrum of **9** in CDCl_3 .

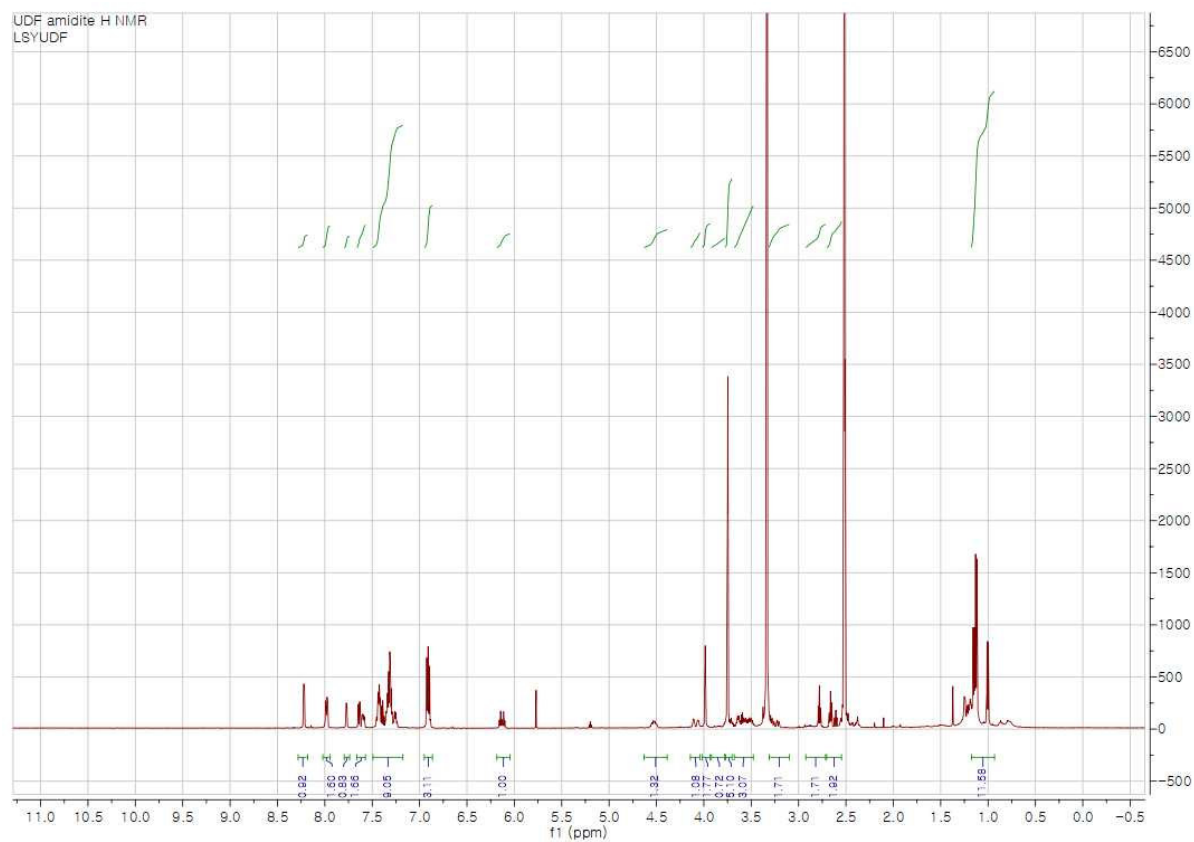


Fig. S11. ^1H NMR spectrum of **10** in $\text{DMSO}-d_6$.